Gypsum Effect on the Aggregate Size and Geometry of Three Sodic Soils Under Reclamation

I. Lebron*, D. L. Suarez, and T. Yoshida

ABSTRACT

Reclamation of sodic soils is imperative in many areas where deterioration of land and water resources is in progress. While the chemical mechanisms involved in the reclamation of sodic soils are well described and understood, the in situ physical processes undergoing during the salt leaching and cation substitution are normally not taken into consideration. Three sodic soils mixed with different amounts of gypsum were packed in columns and leached under saturated conditions for a period of time between 1 and 3 mo. Saturated hydraulic conductivity (K_{sat}) was measured and a thin section was prepared for each of the columns. We used scanning electron microscopy (SEM) and image analysis to measure the size and shape of the aggregates and the pores, and correlated these with chemical and physical parameters. We divided the area by the perimeter (A/P) to quantify the size and A/P^2 to express geometry for both aggregates and pores. The size of the aggregates had a good correlation with the exchangeable Na percentage (ESP), bulk density, pore size, and K_{sat}. There was no significant relationship between pore size and texture, indicating that transport models using particle-size distribution to infer porosity may not be successful in predicting water transport in soils under reclamation. The linear relationship between aggregate size and pore size indicates that the pore space is determined by the packing of the aggregates not the individual particles, this relationship may have implications not only for water transport but for modeling hydraulic properties in general.

The need for reuse of secondary waters in agriculture generates a demand for tools to predict the long term impact that those waters will have on the soil structure. Models exist to simulate sodification and reclamation scenarios, one of these models, UNSATCHEM (Simunek and Suarez, 1996), also simulates, based on a regression of the variables against saturated hydraulic conductivity, the effect of the water composition on hydraulic properties. With this program, we can estimate the time as well as the amount of water needed to obtain a given ESP in soils using different amendments. In these calculations UNSATCHEM considers the cation affinities of the exchangeable complex of specific clays, kinetics of the dissolution and precipitation of different minerals, fluctuations of CO_2, and changes in pH.

While the chemical reactions involved in soil sodification and reclamation are relatively well known, there is no direct information, to our knowledge, about the physical mechanisms taking place in the soil while these processes are occurring. Changes in soil structure are quantified with reduction functions or simple correlations, but they typically do not explicitly account for the effect of solution chemistry on the arrangement of the soil particles and aggregates. Dispersion or flocculation of clays occurs because of the repulsion of similar charged clay platelets and the ability of the soil solution to mitigate this repulsion. Irreversible changes in soil structure may occur when clay particles become dislodged if, for example, the electrolyte level is decreased or the Na fraction increases.

There are several studies in which the decrease of K_{sat} has been related with increases in Na content (McNeal and Coleman, 1966; Frenkel et al., 1978; Shainberg and Letey, 1984; Suarez et al., 1984). However, there is no quantification, to our knowledge, of the repercussion that increases (or decreases) of Na have on the soil structure while water flow is occurring. Flocculation, slacking, and aggregate stability studies show that increases in ESP cause dispersion and a decrease in aggregate stability and aggregate size, but these tests are performed in fractions of the soil placed in sieves or test tubes. Despite all the information collected in the laboratory there are some doubts about our capability to predict the extent of aggregation and dislodging in real soils.

Explanation for the clay behavior has been typically based in the Derjaguin, Landau, Verwey and Overbeek (DLVO) model, this theory has been used successfully to explain a great number of laboratory experiments. Unfortunately, there is evidence that the electrical double-layer interactions between charged particles in confined geometries are different than in isolated environments (Larsen and Grier, 1997; Grier, 1998; Bowen and Sharif, 1998; Sader and Chan, 1999). Grier (1998) and Bowen and Sharif (1998) found that isolated pairs of like charged spheres behave as predicted by DLVO theory but spheres confined by a concentration of other spheres develop long-range attractions inconsistent with DLVO.

Dilute systems may not properly represent the soil scenario, as geometrical confinement has a dramatic effect in the pairwise double-layer interaction between two clay particles. Sader and Chan (1999) found that the interaction between two confined spheres with uniform constant surface charge is primarily affected by the electrical nature of confining plates. They also found that when the interaction is between two spheres with uniform constant surface potential, the interaction between the spheres is not only strongly affected by the potential and charge but is also affected by the electrical properties of the confining plates.

Considerations of previous findings summarized above, indicates that there is a need to reevaluate our

U.S. Salinity Laboratory, Riverside, CA. Received 30 Mar. 2001. *Corresponding author (ilebron@ussl.ars.usda.gov).

Published in Soil Sci. Soc. Am. J. 66:92–98 (2002).

Abbreviations: A, area; DLVO, Derjaguin, Landau, Verwey and Overbeek; ESP, exchangeable Na percentage; GR, gypsum requirement; K_{sat}, saturated hydraulic conductivity; P, perimeter; R_h, hydraulic radius SAR, Na adsorption ratio; SEM, scanning electron microscopy.

knowledge of colloidal systems and perform measurements under conditions at which flow and transport phenomena occur. For that purpose, image analysis of soil micrographs has been proven to yield information impossible to collect otherwise.

There is a general agreement that the active pores conducting water are those at the micrometer scale (Ahuja et al., 1989). The size of the particles enclosing such pores are mostly aggregates, which are heterogeneous conglomerates in which submicron-clay particles are associated in domains. These domains are cemented with a variety of amorphous oxides, organic matter, and minerals. Scanning electron microscopy is suitable to measure features at the micrometer scale and together with image analysis provides the quantification required to follow changes in pore and aggregate size and shape with changing chemical and external factors (Lebron et al., 1999).

Gypsum has been used extensively in reclamation of sodic soils with infiltration problems. It is well known that application of gypsum to sodic soils improves the soil physical conditions by promoting flocculation, enhancing aggregate stability and increasing the infiltration rate. These observations have no scientific documentation or quantification regarding the actual assembling of the soil particles at the aggregate level.

Chemical and physical factors that affect soil structure should be considered in predictive and indirect models for the soil hydraulic properties. In the present study, we quantify the changes that the pores and aggregates undergo when a reclamation process with gypsum takes place in a sodic soil. We also relate the changes in size and shape of the aggregates with saturated hydraulic conductivity. This study is intended to establish the basis for a conceptual model to predict soil reclamation, salinization, and sodification processes in soils.

MATERIALS AND METHODS

Calculations of the gypsum requirement were made considering the cation exchangeable complex of the clays, exchange efficiency, and the initial and final ESP using the gypsum requirement (GR) equation described by Oster and Jayawardane (1998):

$$GR = 0.00086 F D_s \rho_b (CEC)(ESP_i - ESP_f) \quad [1]$$

where GR is the gypsum requirement, F is a Ca-Na exchange efficiency factor and for this case was considered equal to 1, D_s is the depth of the soil to be reclaimed, ρ_b is the soil bulk density, CEC is the cation-exchange capacity, and ESP_i and ESP_f are the initial and final exchangeable Na percentage.

Three saline-sodic soils were collected to measure the effect of gypsum on the soil structure and K_{sat}: Hanford (coarse-loamy, mixed, superactive, nonacid, thermic Typic Xerorthents) loamy sand (H) and Madera (fine, smectitic, thermic Abruptic Durixeralfs) sandy clay loam (M) from Madera County, CA, and Las Animas (coarse-loamy, mixed, superactive, calcareous, mesic Typic Fluvaquents) silty loam (LA) from Arkansas Valley, CO. A total of 24 soil columns were prepared as follows: from the Hanford soil, three different soil samples were collected, each one of the three samples was divided into four subsamples and treated with a GR of 0, 0.3, 0.5, and 1. Madera soils were divided into three subsamples and treated to achieve GR of 0, 0.3, and 0.5. Las Animas soils were divided into three subsamples and these were treated with 0.3, 0.5, and 1.0 of GR. The original ESP values of the samples were between 43 and 54.

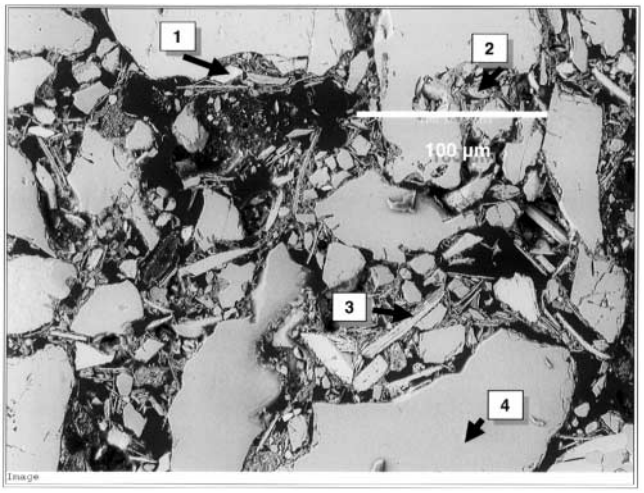

Fig. 1. Thin section micrograph from soil in Column 9. Multipoint chemical analysis using energy dispersive x-ray analysis (EDXA) is marked with arrows, chemical results are as follows(the percentages are noted SiO_2, Al_2O_3, CaO, K_2O, and FeO, respectively): No. 1., 56.02, 10.16, 9.43, 3.51, 20.30; No. 2., 60.70, 24.23, 2.85, 7.84, 4.19; No. 3., 60.20, 15.57, 2.03, 7.57, 14.01; and No 4., 96.62, 1.34, 0.78, 0.77, 1.19.

Soils were mixed thoroughly with the gypsum and packed in columns of 5-cm diam. by 18 cm long to bulk densities between 1.6 to 1.3 g cm^{-3}. Samples were saturated by first wetting by capillarity rise from below, then gradually raising the water level until water ponded on the surface. A constant head was used to measure K_{sat}. Leaching was achieved using Riverside municipal water. The chemical composition of the water was in the range of electrical conductivity (EC) = 0.51 to 0.56 dS m^{-1}, Na adsorption ratio (SAR) = 0.3 to 1.7, and pH = 8.3 to 7.8. A minimum of 1 mo and a maximum of 3 mo was taken for each of the reclamation process, at least three pore volumes were allowed to pass through each column. Slow infiltration rates were used to realistically simulate field reclamation. Infiltration rates were measured and K_{sat} was calculated. At the end of the leaching process a 2-cm thick slide was cut from the top of the column; this slide was used to prepare a thin section. The slide was impregnated with an epoxy, after the preparation was hard, a thin section was cut and polished. Thin section preparation and SEM methodology is explained in detail in Lebron et al. (1999). Image analysis software was used to quantify the pore space and the aggregate dimensions (Princeton Gamma Tech.[1], Princeton, NJ). The magnification used to collect the microscopic information was ×50, that magnification provides pictures of 1024 by 804 pixels at 5.588 μm per pixel. Ten pictures from the same thin section were collected following a grid pattern and appended in one file. For each thin section a total of 46 mm^2 was sampled.

The aggregates were quantified by directly measuring the number of pixels that conform to each feature in the binary image. Figure 1 shows the micrograph of a thin section with the gray scale produced by the electron reflection of the components of the soil. The electron reflection is proportional to the atomic weights of the chemical elements from the minerals

[1] Trade names and company names are included for the benefit of the reader and do not imply any endorsement or preferential tratment of the product listed by the USDA.

Table 1. Texture, $CaCO_3$, organic matter (OM), cation-exchange capacity (CEC), and exchangeable Na percentage (ESP) of the soils in their natural conditions. Electrical conductivity (EC), Na adsorption ratio (SAR) and pH were measured in the saturated paste before the start of the experiment.

Soil type	Sand	Silt	Clay	$CaCO_3$	OM	EC	CEC	ESP	SAR	pH
		%				dSm^{-1}	$mmol_c\ kg^{-1}$			
Hanford	78.96	14.78	6.26	0.07	0.41	10.44	59.2	46.6	45.2	7.06
La Animas	31.97	50.76	17.27	6.04	1.27	12.08	145	54.5	44.5	8.10
Madera	52.40	25.74	22.22	0.06	0.61	10.57	150	45.3	43.0	7.64

of the soil. When Fig. 1 is transformed to binary colors with image analysis, the image is transformed to black and white. White areas represents the aggregates and black represents the pores, both of them were quantified by counting the pixels conforming each feature.

Saturated pastes were prepared for all the soil columns after the reclamation process was finished. Cations and anions were determined in the extract of the saturated paste by inductively coupled plasma (cations and S) or titration (alkalinity and chlorides). Electrical conductivity and pH were also measured in the saturation extract.

A portion of the saturated paste was used to equilibrate and exchange the cations with NH_4NO_3 solution. The supernatant solution after equilibration was analyzed for alkalinity, SO_4^{2-}, Cl^-, Ca^{2+}, Mg^{2+}, Na^+, and K^+. Three corrections were taken into account to express the final results: (i) the correction because of the carryover was calculated based on Cl data, (ii) the correction for calcite dissolution was made with alkalinity data, and (iii) the correction for gypsum dissolution with SO_4^{2-} data (Amrhein and Suarez, 1990). Final composition for the exchangeable complex was calculated and expressed as CEC or ESP.

Aggregate stability was determined in four soils using the method of Kemper and Rosenau (1986). The soils samples were collected from the Columns 9, 10, 20, and 21 after the reclamation process was finished. In this method, only one fraction of the soil is tested (aggregates between 1 and 2 mm) and the sieves contained stainless steel 0.26-mm screens (24 mesh cm^{-1}). Each sample was run in duplicate.

We used the Spearmen correlation (Press et al., 1988) to calculate the relationship among the different variables of our soils. We used this technique because of the fact that our data are not normally distributed, we chose two levels of significance, 0.05 and 0.01.

The clay fraction (<2 μm) was collected from the soils. X-ray diffraction (XRD) was performed on a randomly oriented powder preparation and in two glass slides, one with the clay sample saturated with K and the other with the clay saturated with Mg in 10% glycerol and at 10% humidity (Whittig and Allardice, 1986).

We also used energy dispersive X-ray analysis (EDXA) to analyze the elemental composition in the thin sections of different aggregates in selected samples. This analysis was intended to clarify the composition of the aggregates between 10 and 30 μm.

RESULTS AND DISCUSSION

The soil structure was directly affected by the solution composition. This study presents basic microscopic information of the aggregate size and shape of three sodic soils in which ESP has been modified using gypsum as an amendment. The initial chemical properties for the three soils: ESP, calcite, and organic matter content as well as EC and pH from the saturated paste, are shown in Table 1. The clay minerals present in the soils are a mixture of mica, kaolinite, chlorite, and small amounts of smectite. Las Animas soil has a greater smectite content, estimated at 20%. There was a wide range in the texture of the soils. All soil samples were initially saline and sodic (ESP > 15 and EC of the extract >4.0 dS m^{-1}).

After application of the gypsum and leaching the columns, all the EC values were below 2 dS m^{-1} (Table 2), what is not traditionally considered as saline (U.S. Salinity Laboratory, 1954). The ESP also decreased with respect to the original values, but the reduction in ESP varied depending upon the GR and the soil texture. Table 2 shows the chemical analysis of all the soils columns after the reclamation process was finished.

The pH values in Table 2 show an increase with respect to the original soils (Table 1). The increase in pH is more relevant in the columns belonging to Las Animas soil, which has the greater calcite content. Analysis of the organic matter in Las Animas soil before and after the reclamation process showed a decrease in organic matter from 1.4 to 0.77%, this decrease is consistent with the highly colored effluent obtained during the leaching of this soil. No changes with respect to the

Table 2. Type of soil (H for Hanford, LA for las Animas, or M for Madera; the number after the type of soil indicates the sample 1, 2, or 3), gypsum requirement (GR) (0, 0.3, 0.5, or 1 GR), and amount of gypsum added in each column. The electrical conductivity (EC) and pH were measured at the end of the experiment in a saturated paste. Sodium adsorption ratio (SAR) values correspond to the last effluent from the column, exchangeable Na percentage (ESP) was determined also after the K_{sat} was performed. Data shown as – are missing data.

No.	Soil	GR	Gypsum	EC	pH	SAR	ESP	K_{sat}
			$g\ kg^{-1}$	dSm^{-1}				$cm\ d^{-1}$
1	H1	0.0	0.00	0.66	7.88	8.3	10.2	0.3238
2	H1	0.3	0.11	0.56	7.81	2.1	2.6	0.3658
3	H1	0.5	0.19	0.58	7.84	2.0	2.3	0.7171
4	H1	1.0	0.38	0.60	7.80	2.0	2.2	0.8810
5	H2	0.0	0.00	0.51	7.72	2.6	2.8	0.2746
6	H2	0.3	0.11	0.55	7.64	2.1	2.2	0.4243
7	H2	0.5	0.19	0.61	7.63	2.0	2.1	0.5587
8	H2	1.0	0.38	0.63	7.73	2.1	2.2	0.9360
9	H3	0.0	0.00	0.54	7.68	2.5	2.7	0.2405
10	H3	0.3	0.11	–	–	2.0	2.3	0.3182
11	H3	0.5	0.19	0.57	7.87	2.1	2	0.5321
12	H3	1.0	0.38	0.60	8.00	1.9	2.3	0.8782
13	LA1	0.0	0.00	1.53	8.56	21.1	53.4	0.0242
14	LA1	0.3	0.27	1.44	8.54	21.0	46.0	0.0257
15	LA1	0.5	0.46	0.99	8.21	14.9	26.8	0.0252
16	LA2	0.0	0.00	1.05	8.22	15.0	24.9	0.0250
17	LA2	0.3	0.27	0.91	8.22	13.0	23.2	0.0456
18	LA2	0.5	0.46	0.92	8.21	13.0	22.6	0.0384
19	M1	0.3	0.27	1.01	7.96	22.7	29.6	0.0055
20	M1	0.5	0.46	1.12	8.15	24.2	30.7	0.0058
21	M1	1.0	0.91	0.88	8.03	20.9	26.7	0.0041
22	M2	0.3	0.27	0.92	7.50	15.3	19.9	0.0098
23	M2	0.5	0.46	0.92	7.03	6.4	8.9	0.0300
24	M2	1.0	0.91	0.92	7.50	5.7	9.0	0.0360

Table 3. Spearman rank correlation between variables porosity (Φ), bulk density (ρ_b), hydraulic radius (R_h), aggregate area divided by aggregate perimeter $(A/P)_a$, pore shape factor $(A/P^2)_p$, exchangeable Na percentage (ESP), Na adsorption ratio (SAR), and pH. We chose two levels of significance, * corresponds to the 0.05 level and ** to the 0.01.

	Φ	ρ_b	R_h	$(A/P)_a$	$(A/P^2)_p$	ESP	SAR	pH	K_{sat}
Φ	1								
ρ_b	−0.0538	1							
R_h	0.0278	0.8800**	1						
$(A/P)_a$	−0.2052	−0.8409**	0.7939**	1					
$(A/P^2)_p$	−0.1252	0.8638	0.9026**	0.7704**	1				
ESP	0.0707	−0.6570*	−0.7661**	−0.7845*	−0.6780*	1			
SAR	0.0404	−0.7233**	−0.7947**	−0.8658**	−0.6728*	0.9146*	1		
pH	0.2959	−0.5170	−0.6619*	−0.4308	−0.6906*	0.6288*	0.5584	1	
K_{sat}	0.1530	0.5575	0.6374*	0.7122**	0.4322	−0.8874**	−0.9118**	−0.3433	1

organic C during the reclamation was observed for the other two soils.

The soils after the reclamation process showed a linear relationship between EC and ESP (Table 3). In this particular case, the final EC is relatively low for all the samples, consequently we will consider the dispersion to be controlled by the SAR levels.

We used image analysis to quantify from micrographs, the size and characteristics of the aggregates and the pores from soil columns where gypsum was added. Some of the aggregate and pore parameter data are shown in Table 4. Since the soil aggregates do not have a well-defined geometry, we defined the parameter area, A, divided by perimeter, P, to represent the size of the aggregates. Aggregate size, $(A/P)_a$, was correlated with the Na content, the greater the SAR, the smaller the aggregate size; it was also inversely correlated with the bulk density (ρ_b) (Table 3).

The presence of gypsum reduced the ESP of the soils. Table 2 shows that, for the same soil, the level of reclamation depended upon the different amounts of gypsum added. As we said before, this reduction in ESP was associated with bigger aggregate sizes. Figure 2 shows the increase in the area of the aggregates with decreasing ESP, these two variables are related by a power relationship in which the inflection of the curve coincides with ESP values in the range of 5 to 15. Exchangeable Na percent of 5 to 15 is traditionally the range of values that appear in the literature as the threshold at which tactoids or clay domains break apart.

For the same soil, the bulk density was the same for all the gypsum requirements at the beginning of the experiment (Table 4), however, for Hanford and Madera soils, some compaction occurred during the leaching. The column with the greater gypsum requirement showed less compaction than the columns with less gypsum requirement, the less gypsum, the more compaction. Data in Table 4 indicates that all the aggregates in Hanford and Madera soils underwent a breakdown as the leaching was occurring. The gypsum in the columns prevented, to some extent, this aggregate breakdown. Figure 3 shows the aggregate-size distribution for Columns 9 and 12. We see that the distribution is very similar for both samples, which is not surprising, since they represent the same soil with different gypsum amendments, however, for Column 9 there is a slight enrichment in the quantity of aggregates 10 to 30 μm. The enrichment in the fraction of 10- to 30-μm aggregates in

Table 4. Area (A), perimeter (P), and average diameter (D_{aver}) for aggregates and pores measured using image analysis on micrographs. The >300 (%) corresponds to the weighted percentage of the aggregates >300 μm. Also is shown the porosity (Φ), and bulk density before (ρ_{bi}) and after (ρ_{bf}) perform the leaching process.

No.	Aggregates (μm)				Pores (μm)			Φ	ρ_{bi}	ρ_{bf}
	A	P	D_{ave}	>300 (%)	A	P	D_{ave}	%	g cm^{-3}	g cm^{-3}
1	10 804	414	64	90.5	2 496	277	57	23.8	1.44	1.63
2	14 058	417	60	87.6	2 286	260	55	24.0	1.44	1.63
3	11 702	349	59	89.3	2 033	255	54	19.8	1.44	1.61
4	12 799	397	60	89.0	2 403	275	56	22.0	1.44	1.57
5	10 237	358	60	89.6	2 700	278	57	22.7	1.44	1.61
6	10 121	336	54	85.9	1 711	229	50	19.5	1.44	1.61
7	14 603	380	61	89.9	2 530	269	55	22.8	1.44	1.61
8	11 096	389	60	90.3	2 667	293	57	22.4	1.44	1.57
9	7 535	359	60	89.7	2 605	281	56	27.1	1.44	1.61
10	10 804	313	55	86.4	2 302	248	51	20.3	1.44	1.63
11	12 505	386	60	90.0	2 046	250	53	20.6	1.44	1.59
12	12 405	351	56	87.0	2 015	257	55	20.6	1.44	1.55
13	323	61	10	75.0	48	43	9.5	23.9	1.34	1.31
14	340	62	9.7	75.6	45	42	9.5	23.4	1.34	1.31
15	309	53	9.5	76.2	48	42	9.4	24.3	1.34	1.28
16	258	60	9.6	74.0	44	42	9.4	24.2	1.34	1.28
17	185	53	9.4	75.3	44	41	9.3	23.6	1.34	1.27
18	407	67	10	75.1	42	40	9.1	21.4	1.34	1.27
19	452	51	9	83.9	60	43	9	19.3	1.35	1.43
20	613	63	11	83.6	59	45	10	19.2	1.35	1.43
21	389	55	9	83.3	63	46	12	19.4	1.35	1.47
22	655	52	9	86.4	62	44	10	18.7	1.35	–
23	203	48	9	82.9	68	47	10	22.4	1.35	1.42
24	311	52	9	80.1	64	47	10	19.7	1.35	1.40

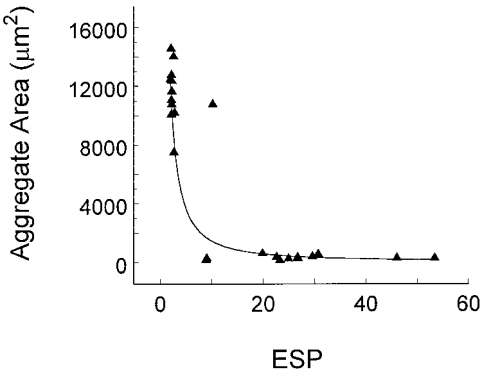

Fig. 2. Area of the aggregates as a function of the exchangeable Na percentage (ESP).

the soil without gypsum corresponds with an equivalent decrease in the number of aggregates >50 μm. A chemical analysis of selected particles in the micrographs shows that the majority of the 10- to 30-μm aggregates in the soils without gypsum are phyllosilicates of different mineralogy (Table 5, Points 1, 2, and 3 from Fig. 1). Quartz was, in general, predominant in the particles >60 μm (Table 5, Point 4).

The interpretation of the breakdown and formation of aggregates can be made based on an in situ study of the effect of wetting and drying on aggregates (Silva, 1995) and the model of Ghezzehei and Or (2000), in which they modeled the dynamics of soil aggregate dislodging and coalescence. According to Ghezzehei and Or (2000) when the soil is at saturated conditions the aggregates go through a softening of the strength holding the particles and possibly dislodging but, under such wet conditions, the coalescence of two or more particles to generate new aggregates is unlikely. Coalescence of particles occurs during the drying process.

Since our experiment was performed under saturated conditions, the presence of gypsum in our columns is supposed to act by inhibiting the breakdown of the already existing aggregates rather than promote the formation of larger ones. That inhibition occurs by increasing the Ca concentration in the bulk water and promoting the exchange of Na by Ca in the exchangeable complex of the clays. Only at the end of the experiment, in the drying process of the soil columns, can we expect new aggregate formation.

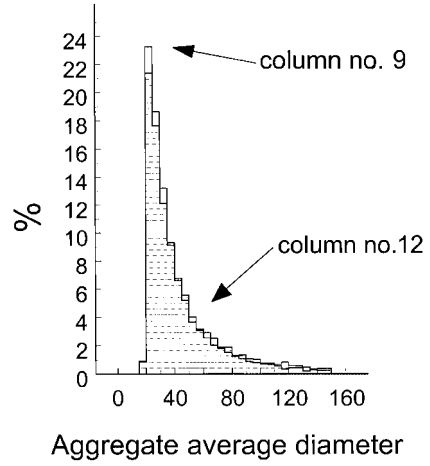

Fig. 3. Aggregate-size distribution for Hanford Soil 3 when 1 gypsum requirement (GR) was added (Column 12) and when no gypsum was added (Column 9).

Table 5. Multipoint analysis (1, 2, 3, and 4 shown in Fig. 1) using energy dispersive spectroscopy X-ray technique (EDXA).

%	1	2	3	4
SiO_2	56.02	60.70	60.20	96.62
Al_2O_3	10.16	24.23	15.57	1.34
CaO	9.43	2.85	2.03	0.78
K_2O	3.51	7.84	7.57	0.77
FeO	20.30	4.19	14.01	1.19

At the soil water content of saturation the disruption of the aggregates in the soil matrix is to a certain extent irreversible. Once the aggregate is broken, the individual particles will migrate if they are not physically constrained. The experiment lasted long enough to show some compaction when gypsum was not present and since the soil did not go through drying periods no significant amount of new aggregates should form during the leaching (Ghezzehei and Or, 2000). The beneficial effect of the gypsum is shown not only by the greater K_{sat}, but also by the lower bulk densities at the end of the experiment in comparison with their homologous soil with less or no gypsum. Las Animas soil shows some initial swelling because of the presence of small amounts of smectite clay but it shows a similar pattern; the greater the gypsum requirement the less the compaction during the leaching; the columns with the lower GR showed higher ρ_b.

The losts of soil structure, however, was not as much as we could have predicted from traditional aggregate stability tests. The results from Kemper and Roseanu method showed a percentage of the stable aggregates of 52.71 (±1.46), 57.54 (±2.60), 24.5 (±1.43), and 26.2 (±0.25) for Columns 9, 10, 20, and 21. We analyzed the weighted percentage of the aggregates in our thin sections. Table 4 shows that the aggregates between 0.3 and 2 mm were between 80 and 90% for Hanford and Madera soils. Since each micrograph has 46 mm^2 and there were always more than two aggregates in each picture, we can safely assume that the maximum aggregate size analyzed with the SEM is similar to the one analyzed with the Kemper and Rossenau method (2 mm in diam.).

Aggregate stability test may not be reflecting the actual stability of the particles when they are constrained by the physical confinement of the soil matrix. The complexity of the electric field of the colloids overlapping and interacting in enclosed geometries has been shown to not follow the DLVO theory. Our soils show a more stable status than the one that would have been predicted according with experiments in dilute systems in which DLVO theory is applicable. The presence of long range attractive forces observed at length scales of several micrometers (Larsen and Grier, 1997; Squires and Brenner, 2000) and the fact that the aggregate stability tests are performed with loose soil after sieving and handling can be the reasons for the discrepancies shown between the traditional method and the in situ microscopic measurements.

Soil pores, as is the case with aggregates, do not have a specific geometry. Some authors utilize the hydraulic radius, what Hoffmann-Riem et al. (1999) defined as the ratio between the volumetric water content and the area of the water-solid interface. In our case, we used the hydraulic radius (R_h) defined as the area divided by the perimeter, Lebron et al. (1999) showed that R_h improved the capability to predict K_{sat} using the Kozeny-Carman equation when A and P were measured directly from a micrograph of a thin section.

The R_h was found to have a good correlation with all the chemical parameters and with K_{sat} (Table 3). These observations agreed with previous data in the literature (Lebron et al., 1999). The greater the ESP or the pH, the smaller the pores and consequently the lesser the K_{sat}. The R_h also had a good correlation with the ρ_b but it did not show any correlation with the total porosity (Φ) (Table 3).

We observed that $(A/P)_a$ had a linear relationship with R_h indicating that the size of the pores is determined by the size of the aggregates. This relationship seems intuitive and is one of the main conclusions of the present study. Unlike most of the previous modeling efforts we propose to concentrate on the aggregate size and distribution rather than on the texture to evaluate the pore space in soils. No relationship was found between pore size and texture. Lebron et al. (2001) also found a relationship between pore size and aggregate size for undisturbed soil cores. They proposed that the transformation of the texture data into aggregate size considering the chemistry and bulk density of the soils will improve the capability to predict hydraulic properties in soils.

Pore and aggregate size is critical but their shapes are also important (Philip, 1977; Reeves and Celia, 1996). A important feature of the pore structure in a real porous media is the angular corners of the pores. Ma et al. (1996) proposed a model of angular tubes as opposed to the commonly used cylindrical tube model to represent soil pore space. Triangles provide a versatile example for pore shapes; they have angular corners which can retain liquid, and irregular triangles give a wide range of shapes (Manson and Morrow, 1991). Manson and Morrow (1991) proposed a normalized shape factor for capillary action in triangular pores given the ratio between the cross-sectional area, A, to the square of the perimeter length, P. According to these authors, the amount of wetting phase that drains as the penetration curvature decreases as aspect ratio increases. The shape factor, A/P^2, has been successfully used by Tuller et al. (1999), Lebron et al. (1999), and Or and Tuller (1999, 2000).

As shown in Table 3, A/P^2 has a good correlation with ESP, SAR, and pH. This indicates that the chemical composition had an effect on the shape of the pores. Gypsum affected soil structure, not only the size of the aggregates but also in the self assembling of the particles, since the shapes of the pores were altered. The greater the pH or Na content the lesser the shape factor. These results are in agreement with Manson and Morrow (1991) and with our previous experiments (Suarez et al., 1984; Lebron et al., 1999) in which increases in ESP or pH causes a decrease in the water flow draining from a soil column.

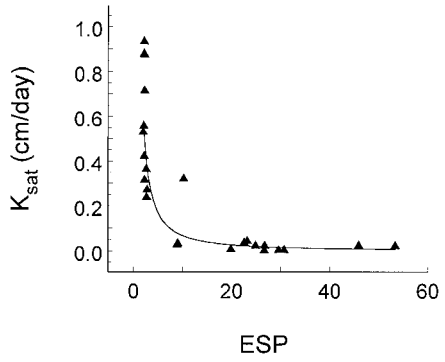

Fig. 4. Relationship between exchangeable Na percentage (ESP) and saturated hydraulic conductivity (K_{sat}) for Hanford, Las Animas, and Madera soils.

From Table 3, we see also that K_{sat} had a good correlation with several physical and chemical parameters. Some of these interactions, such as the effect of exchangeable Na on the permeability (Fig. 4) of soils, have been known for a long time (Hilgard, 1890). However, incorporation of chemical parameters in the physical models to predict water transport has not been achieved. For example, K_{sat} was found to have a good correlation with the aggregate size $(A/P)_a$ (Fig. 5), since aggregate size is affected by the chemical composition, one way to conceptually develop a model to predict K_{sat} would be to calculate the aggregate size based on the chemical composition. This process would require the accumulation of a large data base with microscopic, macroscopic, and chemical information to be able to develop the relationships linking the different variables. Variables such as clay mineralogy, organic matter, and Al and Fe oxides, all known to affect the stability of the soils should be included in the data base to obtain relationships applicable to a wide range of soils.

The microscopic technique used in this work shows that we can quantify changes in the aggregate and pore

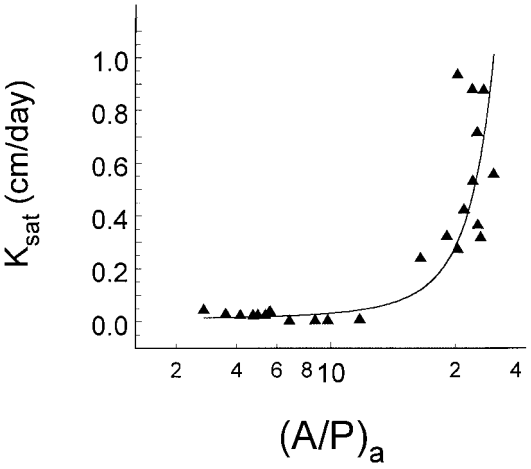

Fig. 5. Relationship between aggregate size expressed as aggregate area, *A*, divided by aggregate perimeter, *P*. Both *A* and *P* were measured in the micrographs using image analysis.

characteristics when changing chemical conditions. It has been shown that microscopic measurements of the aggregates are correlated with chemical parameters. To infer aggregate size from easy to measure parameters (i.e., SAR, pH, texture, etc.) it is necessary to create a data base in which, information from a substantial numbers of soils would allow us to apply techniques such as neural network analysis to calculate the nonlinear relationships linking all the variables. This data base will be required before we are able to predict structural changes and ultimately incorporate this information into transport models.

CONCLUSIONS

The presence of gypsum in soil columns prevented the breakdown of aggregates in proportion to the amount of gypsum added. The more gypsum the less breakdown of aggregates. A shape factor for aggregates and pores decreased when ESP or pH increased indicating that chemical conditions affected not only the size but the self arrangement of the aggregates in the soil matrix. However, the stability of the aggregates was greater than we would expect from traditional tests of aggregate stability. The discrepancy between the traditional laboratory methods and the microscopic method presented in this work may be because of the fact that our method quantifies aggregate and pore properties in situ, and consequently the effect of the soil matrix in the physical confinement of the aggregates and possibly the effect of long distance attractive forces are taken into consideration. The size of the pores was found to be correlated with the size of the aggregates and not with soil texture.

REFERENCES

Ahuja, L.R., D.K. Cassel, R.R. Bruce, and B.B. Barnes. 1989. Evaluation of spatial distribution of hydraulic conductivity using effective porosity data. Soil Sci. 148:404–411.

Amrhein, C., and D.L. Suarez. 1990. A procedure for determining sodium-calcium selectivity in calcareous and gypsiferous soils. Soil Sci. Soc. Am. J. 54: 999–1007.

Bowen, W.R., and A.O. Sharif. 1998. Long-range electrostatic attraction between like-charge spheres in a charged pore. Nature 393: 663–665.

Frenkel, H., J.O. Goertzen, and J.D. Rhoades. 1978. Effects of clay type and content, exchangeable sodium percentage, and electrolyte concentration on clay dispersion and soil hydraulic conductivity. Soil Sci. Soc. Am. J. 42:32–39.

Ghezzehei, T.A., and D. Or. 2000. Dynamics of soil aggregate coalescence governed by capillary and rheological processes. Water Resour. Res. 36:367–379.

Grier, D.G. 1998. A surprisingly attractive couple. Nature 393:621–623.

Hilgard, E.W. 1890. Alkali lands, irrigation and drainage in their natural relations. p. 7–56 *In* California Agr. Exp. Stn. Annual Rep. Appendix. Sacremento State Office. State Printing, Sacremento, CA.

Hoffmann-Riem, H.H., M.Th. van Genuchten, and H. Fluher. 1999. A general model of the hydraulic conductivity of unsaturated soils. p. 31–42. *In* M. Th. van Genuchten et al. (ed.) Characterization and Measurement of the Hydraulic properties of Unsaturated Porous Media. Part 1. Univ. of Calif. Press, Berkeley, CA.

Kemper, W.D., and R.C. Rosenau. 1986. Aggregate stability and size distribution. p. 425–442. *In* A. Klute (ed.) Methods of soil analysis. Part 1, 2nd ed. Agron. Monogr. 9, ASA and SSSA, Madison, WI.

Larsen, A.E., and D.G. Grier. 1997. Like-charge attractions in metastable colloidal crystallites. Nature 385:230–233.

Lebron, I., and D.L. Suarez. 1992. Variations in soil stability within and among soil types. Soil Sci. Soc. Am. J. 56:1412–1421.

Lebron, I., M.G. Schaap, and D.L. Suarez. 1999. Saturated hydraulic conductivity prediction from microscopic pore geometry measurements and neural network analysis. Water Resour. Res. 35:3149–3158.

Lebron, I., M.G. Schaap, and D.L. Suarez. 2000. Soil pore space as affected by sodium. p. 212 *In* Annual Meeting Abstracts. ASA, CSSA, and SSSA, Madison, WI.

Ma, S., G. Mason, and N.R. Morrow. 1996. Effect of contact angle on drainage and imbibition in regular polygonal tubes. Colloids and Surfaces A. Physicochemical and Engineering Aspects 117:273–291.

Manson, G., and N.R. Morrow. 1991. Capillary behavior of a perfectly wetting liquid in irregular triangular tubes. J. Colloid Interface Sci. 141:262–274.

McNeal, B.L., and N.T. Coleman. 1966. Effect of solution composition on soil hydraulic conductivity. Soil Sci. Soc. Am. Proc. 30:308–312.

Or, D., and M. Tuller. 1999. Liquid retention and interfacial area in variably saturated porous media: Upscaling from single-pore to sample-scale model. Water Resour. Res. 35:3591–3606.

Or, D., and M. Tuller. 2000. Flow in unsaturated fractured porous media: Hydraulic conductivity of rough surfaces. Water Resour. Res. 36:1165–1177.

Oster, J.D., and N.S. Jayawardane. 1998. Agricultural management of sodic soils. p. 125–147. *In* M.E. Sumner and R. Naidu (ed.) Sodic Soils. Oxford University Press, New York.

Philip, J.R. 1997. Adsorption and geometry: The boundary layer approximation. J. Chem. Phys. 67:1732–1741.

Reeves, P.C., and M.A. Celia. 1996. A functional relationship between capillary pressure, saturation, and interfacial area as revealed by a pore-scale network model. Water Resour. Res. 32:2345–2358.

Sader, J.E., and D.Y.C. Chan. 1999. Electrical double layer interaction between charged particles near surfaces and in confined geometries. J. Colloid Interface Sci. 218:423–432.

Shainberg, I., and J. Letey. 1984. Response of soils to sodic and saline conditions. Hilgardia 52:1–57.

Silva, H.R. 1995. Wetting-induced changes in near surface soil physical properties affecting surface irrigation. Ph.D. diss. Utah State University, Logan, UT.

Simunek, J., and D.L. Suarez. 1996. UNSATCHEM Code for simulating the one-dimensional variably saturated water flow, heat transport, carbon dioxide production and transport, and multicomponent solute transport with major ion equilibrium and kinetic chemistry. Part A. U.S. Salinity Lab. Res. Rep. 128. U.S. Salinity Lab. and USDA, Riverside, CA.

Squires, T.M., and M.P. Brenner. 2000. Like-charge attraction and hydrodynamic interaction. Phys. Rev. Lett. 85:4976–4979.

Suarez, D.L., J.D. Rhoades, R. Lavado, and C.M. Grieve. 1984. Effect of pH on saturated hydraulic conductivity and soil dispersion. Soil Sci. Soc. Am. J. 48:50–55.

Tuller, M., D. Or, and L.M. Dudley. 1999. Adsorption and capillary condensation in porous media: Liquid retention and interfacial configurations in angular pores. Water Resour. Res. 35:1949–1964.

U.S. Salinity Laboratory Staff. 1954. Diagnosis and improvement of saline and alkali soils. USDA Handb. 60. U.S. Gov. Print. Office Washington, DC.

Whittig, L.D., and W.R. Allardice. 1986. X-ray diffraction Techniques. p. 331–362. *In* A. Klute (ed.) Methods of Soil Analysis. Part 1. 2nd ed. Agron. Monogr. 9. ASA and SSSA, Madison, WI.